









Formulation and optimization of polymeric nanoparticles loaded with riolozatrione: a promising nanoformulation with potential antiherpetic activity

GUADALUPE Y. SOLÍS-CRUZ¹ 
ROCÍO ALVAREZ-ROMAN¹ 
VERÓNICA M. RIVAS-GALINDO¹ 
SERGIO ARTURO GALINDO-RODRÍGUEZ² 
DAVID A. SILVA-MARES¹ 
IVÁN A. MARINO-MARTÍNEZ^{3,4} 
MAGDALENA ESCOBAR-SAUCEDO¹ 
LUIS A. PÉREZ-LÓPEZ^{1*} 

¹ Autonomous University of Nuevo Leon, Faculty of Medicine, Department of Analytical Chemistry Monterrey 66460, Nuevo León, México

² Autonomous University of Nuevo Leon, Faculty of Biological Sciences, Department of Chemistry San Nicolás de los Garza, Nuevo León, México

³ Autonomous University of Nuevo Leon, Center for Research and Development in Health Sciences Monterrey 66460, Nuevo León, México

⁴ Autonomous University of Nuevo Leon, Faculty of Medicine, Department of Pathology, Monterrey 66460, Nuevo León, México

ABSTRACT

Riolozatrione (RZ) is a diterpenoid compound isolated from a dichloromethane extract of the *Jatropha dioica* root. This compound has been shown to possess moderate antiherpetic activity *in vitro*. However, because of the poor solubility of this compound in aqueous vehicles, generating a stable formulation for potential use in the treatment of infection is challenging. The aim of this work was to optimize and physicochemically characterize Eudragit[®] L100-55-based polymeric nanoparticles (NPs) loaded with RZ (NPR) for *in vitro* antiherpetic application. The NPs formulation was initially optimized using the dichloromethane extract of *J. dioica*, the major component of which was RZ. The optimized NPR formulation was stable, with a size of 263 nm, polydispersity index < 0.2, the zeta potential of –37 mV, and RZ encapsulation efficiency of 89 %. The NPR showed sustained release of RZ for 48 h with release percentages of 95 and 97 % at neutral and slightly acidic pH, respectively. Regarding *in vitro* antiherpetic activity, the optimized NPR showed a selectivity index for HSV-1 of ≈16 and for HSV-2 of 13.

Keywords: riolozatrione, polymeric nanoparticles, herpes simplex virus, antiviral

Accepted May 4, 2023
Published online May 7, 2023

Herpes simplex virus (HSV) belongs to the Herpesviridae family, and its distinctive feature is its ability to establish lifelong latency in the host and reactivate periodically (1). This virus is a cosmopolitan human pathogen and the second leading cause of human viral illness. It is estimated that about 70 % of the world's population has been infected with herpes simplex virus type 1 (HSV-1) (2). Recent studies have associated HSV-1 neuronal infection with suicidal behavior, psychiatric disorders, and an Alzheimer's-like phenotype (3, 4). On the other hand, herpes simplex virus type 2 (HSV-2) has a global incidence of 24 million new cases per year (5). A strong association between HSV-2 and human immunodeficiency virus infection was recently demonstrated (6).

*Correspondence; email: luis.perezlp@uanl.edu.mx

Most antiherpetic drugs are nucleoside analogs [such as acyclovir (ACV), ganciclovir, and penciclovir] whose mechanism of action is the inhibition of viral DNA replication (7). HSV treatments are effective in reducing clinical manifestations; however, although they can reduce the intensity and frequency of symptoms, they do not cure the infection, and their prolonged use can lead to the development of drug resistance (2). Therefore, new alternatives for treating HSV infections are currently being sought.

The use of plants to combat diseases has been used by humans throughout history (8). Phytochemicals have been the subject of many studies because of their unique structural variability and chemical structures, high therapeutic potential, few side effects, and ability to activate multiple signal transduction pathways (9, 10). Several studies have demonstrated the anti-HSV activities of extracts and pure compounds from various plants. *Jatropha dioica* is a shrub native to Mexico that has reddish branches and produces yellow latex that turns red when oxidized, hence the popular name “sangre de drago” (dragon’s blood). It is widely used in traditional medicine to treat cancer, relieve eye irritation, and cure oral diseases (11). *J. dioica* has several proven biological activities. The hexane extract of its root has activity against *Escherichia coli*, *Candida albicans*, *Cryptococcus neoformans*, and *Staphylococcus aureus* (12). Moreover, the hydroalcoholic extract of the root of *J. dioica* has moderate antifungal and antiherpetic activity (13, 14). In addition, different diterpenoid-type compounds have been isolated from the *J. dioica* root extract. The diterpenoid riolozatrione (RZ), isolated from the dichloromethane extract of *J. dioica* root (DEJ), has been shown to possess moderate *in vitro* antiherpetic activity (15); however, its biological application has been restricted owing to its limited solubility in aqueous vehicles.

One strategy to solve the problem of poor solubility of active compounds is through the use of nanocarriers (NCs) (16, 17). NCs are nanoscale systems designed for drug delivery. The development of NCs has provided an opportunity to address and treat challenging diseases because they can transport drugs to specific tissues and provide controlled-release therapy (18). In addition, NCs protect drugs from rapid degradation or elimination and improve drug concentrations in target tissues (19). These results improved pharmacokinetics, pharmacodynamics, and reduced toxicity. Polymeric nanoparticles (NPs) are a type of NCs consisting of solid particles formed with polymers, in which the active ingredient or other therapeutic substances are encapsulated, adsorbed, or incorporated into a polymeric matrix (18). NPs have become a useful strategy for delivering natural products with anticancer (19), antimicrobial (20), antiasthmatic (21), and antiherpetic (22) activities. In addition to avoiding the degradation of natural products, NPs have favorable bioavailability with respect to free natural products.

The objective of this study was to investigate the *in vitro* antiherpetic activity of an optimized NPR formulation for vaginal administration and to establish appropriate release profiles to ensure bioavailability or biological application.

EXPERIMENTAL

Materials

The Eudragit[®] L100-55 polymer (1:1 methacrylic acid:ethyl acrylate) was purchased from Evonik Industries (Germany). Dulbecco’s Modified Eagle Medium (DMEM), antibiotic, fetal bovine serum (FBS), and the rest of the reagents used for the *in vitro* tests were from Gibco (USA). For the HPLC method, acetonitrile and HPLC-grade methanol from

J. T. Baker (USA) were used. All other chemicals and solvents used in the study were of analytical grade and obtained from Sigma-Aldrich (Germany) or J. T. Baker.

Cells and viruses

The Vero cell line, ATCC CCL-81, and the viruses HSV-1 strain KOS (ATCC VR-1493D) and HSV-2 strain G (ATCC VR-734) were donated by Miguel Dector (PhD) from the Department of Genetics, School of Medicine, UANL.

Preparation of the extract

Roots of *J. dioica* var. *sessiliflora* were collected from the municipality of Villaldama, Nuevo León, Mexico, and authenticated in the Institutional Herbarium of the Faculty of Biological Sciences, Autonomous University of Nuevo Leon. Dried and pulverized *J. dioica* roots (60 g) were subjected to extraction using dichloromethane (3×1 L) at room temperature with constant agitation for 1 h. The obtained DEJ was filtered and dried *via* evaporation under reduced pressure and had a yield of 2.68 ± 0.18 % (*m/m*).

RZ Purification

RZ was purified following the methodology described by Melchor-Martinez *et al.* with slight modifications, as shown in Fig. 1. (15). DEJ was fractionated on silica gel using low-pressure column chromatography (CC) with dichloromethane/acetone (19:1) as the mobile phase (MP). Five fractions (A-E) were obtained based on thin-layer chromatography (TLC) monitoring results. Fraction D was further fractionated *via* low-pressure CC using three MPs: hexane/ethyl acetate (6:4), hexane/ethyl acetate (4:6), and ethyl acetate. Six fractions (D1-D6) were obtained based on the TLC results, and the D-2 fraction was solubilized with an ethyl ether/petroleum ether solution (4:1). The resulting solution was refrigerated at 4 °C overnight. Finally, the obtained crystals were washed with ethyl ether. Purification of RZ from DEJ exhibited a yield of 3.26 ± 0.09 % (*m/m*). The chemical structure and absolute configuration of RZ have been determined using several methods, including vibrational circular dichroism and X-ray diffraction (15).

Quantification of RZ by HPLC

RZ was quantified as described by Castro *et al.* (23). A Waters Alliance 2695 liquid chromatograph (USA) equipped with a 2996 diode array detector (USA) was used. The analysis was performed on the AccQ-Tag column, with a solution of water and acetonitrile as mobile phase and a flow rate of 0.2 mL min^{-1} in gradient mode. The elution program started with a 50 % acetonitrile percentage that increased linearly to reach 100 % in approximately 35 min; this percentage was maintained for 5 min and then returned to the initial conditions. The injection volume was 5 μL and the column temperature was not controlled. Quantification of RZ was performed at a wavelength of 254 nm. The retention time for RZ was 16.5 min and the limit of detection was $8.54 \mu\text{g mL}^{-1}$.

Preparation, optimization, and characterization of NPs

NPs were obtained using the nanoprecipitation technique developed by Fessi *et al.* with slight modifications (24). Briefly, the Eudragit® L 100-55 polymer and sample (DEJ or RZ) were dissolved in an isopropanol/acetone mixture (1:1). The aqueous phase was then

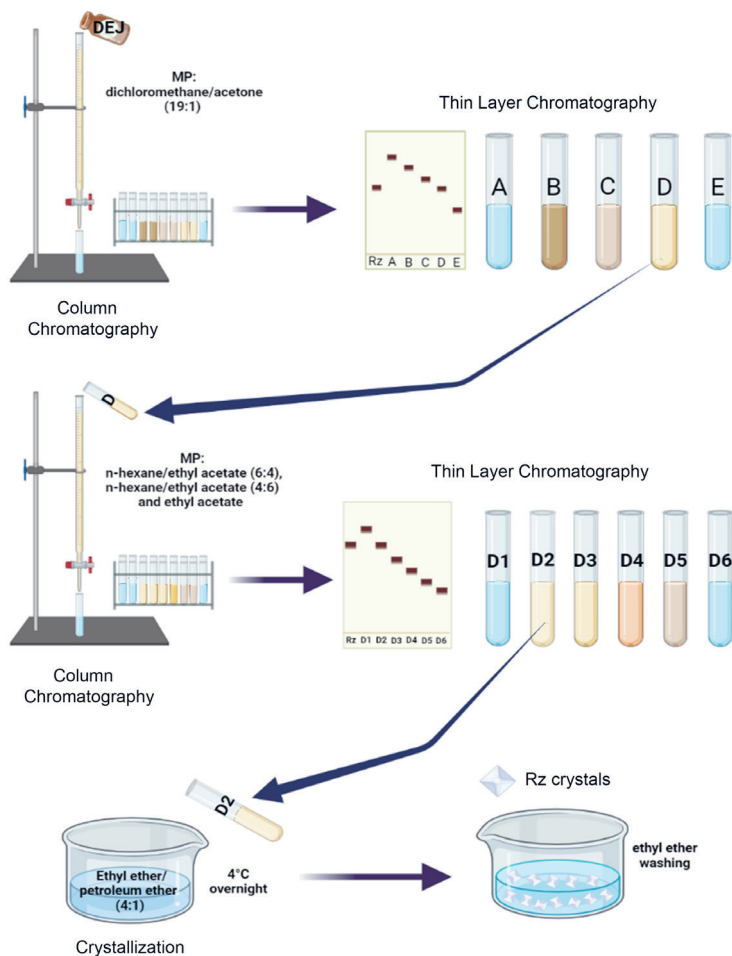


Fig. 1. Isolation and purification of riolozatrione (RZ) from the dichloromethane extract of *J. dioica* root (DEJ).

injected dropwise into the organic phase under constant stirring (250 rpm); the ratio of organic phase to aqueous phase was 1:2. Finally, the organic solvent was evaporated under reduced pressure. In the first step, the formulation of the NPs was optimized with DEJ (NPE), the major component of which was RZ. The DEJ concentration (0.6, 0.84, and 1.4 mg mL⁻¹) and polymer concentration (8 and 14 mg mL⁻¹) were optimized. Once these variables were optimized, RZ-loaded NPs (NPR) were prepared.

Determination of particle size, polydispersity index (PDI), and zeta potential

The size and PDI of the obtained NPs were determined by photon correlation spectroscopy at 90°. The zeta potential was determined using Doppler laser microelectrophoresis.

All determinations were carried out on a Zetasizer Nano Malvern (UK) instrument, and the NPs were dispersed in deionized water (25).

Calculation of encapsulation efficiency and RZ content in NPE and NPR

The content of RZ loaded in the NPE and NPR was determined directly using the previously mentioned HPLC method. The NPs were then centrifuged at 13,000 rpm for 1 h. The sediment was then solubilized in the mobile phase and filtered through a 0.22 μm nylon membrane prior to injection into the chromatography equipment. Each assay was performed in triplicate. The RZ content (RZC) was calculated using Equation 1. The encapsulation efficiency (EE) of RZ was calculated using Equation 2:

$$\text{RZC} = \frac{(\text{encapsulated mg of RZ})}{(\text{mg polymer} + \text{total mg of RZ})} \times 100 \quad \text{Equation 1}$$

$$\text{EE}(\%) = \frac{(\text{encapsulated mg of RZ})}{(\text{total mg of RZ})} \times 100 \quad \text{Equation 2}$$

Stability and residual solvents of nanoparticles

The stability of the NPE aqueous dispersion was evaluated at 6 and 11 months, and that of the NPR aqueous dispersion was evaluated at 6 months. The aqueous dispersions were stored in the dark at 25.47 ± 2.21 °C and relative humidity of 48.65 ± 6.61 %. The stability of the aqueous dispersions was evaluated by visual inspection of the aggregates and sediments. In addition, the particle size, PDI, and zeta potential were measured. The RZCs of the NPR aqueous dispersions were also determined. The presence of residual solvents was determined by gas chromatography-mass spectrometry according to USP guideline 467. The methodology is described in detail in the Supplementary Material (26).

FT-IR analysis

For the FT-IR analysis, 40 scans were performed on each sample in the range of 4000–700 cm^{-1} using a Frontier Optical spectrophotometer (Perkin Elmer, USA). Spectra were obtained for each of the NPR components separately (Eudragit® L100-55 and RZ), as well as for the NPR. Films of NPR were prepared by direct casting of 250 μL of the dispersion onto Teflon plates, followed by a drying time of 12 h at 30 °C (27). Each measurement was performed in triplicate.

In vitro study of riolozatrione release

The release profile was evaluated using the sample-and-separate method (28). For this, 100 μL of an NPR solution containing 10.15 $\mu\text{g mL}^{-1}$ RZ was poured into 900 μL of phosphate- or citrate-buffered medium (pH 7.4 and 4.3 respectively) at a temperature of 37 °C and constant agitation at 150 rpm. RZ release was evaluated at 15 and 30 min, and at 1, 2, 4, 24, and 48 h. Each assay was performed in triplicate. A Microcon® (Merck Milli-

pore[®], Germany) was used to recover the supernatant, which was centrifuged for 30 min at 13000 rpm. Quantification of RZ released from the NPR was performed by UV-visible spectroscopy using a Genesys 10s Thermo Scientific (USA) spectrophotometer at a wavelength of 245 nm. The relative standard deviation was 1.8 % and the detection limit was 1.27 $\mu\text{g mL}^{-1}$.

Cell viability evaluation

Cell viability was determined using the Mossman method with slight modifications (29). To perform the assay, Vero cells were cultured in 96-well plates at a density of 1×10^4 cells/well in DMEM with 2 % FBS. After 24 h, the cells were supplemented with different concentrations of sample to be tested and incubated for 48 h at 37 °C and 5 % CO₂. Vero cells added to only DMEM with 2 % FBS medium were used as negative controls. NPRs were evaluated at concentrations of 11.25, 22.5, 45, 90, 180, and 360 $\mu\text{g mL}^{-1}$ of RZ and NPBco were evaluated at concentrations corresponding to 45, 90, 180, 360, 720 and 1440 $\mu\text{g mL}^{-1}$ of Eudragit[®] L100-55 polymer, respectively. After the incubation period was over, cell viability was determined by adding 10 μL of 3-(4,5-dimethylthiazol-2-yl)-2,5-diphenyl-tetrazolium bromide (MTT) solution at a concentration of 5 mg mL^{-1} per well, incubated 3 h at 37 °C in a 5 % CO₂ atmosphere. The culture medium was removed, and 100 μL of dimethyl sulfoxide was added. Absorbance was measured at 540 nm using a Thermo Scientific Model 357 microplate reader (USA). The cytotoxic concentration 50 (CC₅₀) was determined as the concentration of NPR required to reduce cell viability by 50 % relative to the viability of untreated cells (negative control). The experiments were performed in quadruplicate. In contrast, the percentage of cell viability after the administration of 20 g mL^{-1} of RZ, ACV, NPR (equivalent to 20 g mL^{-1} of RZ), and NPBco at the same polymer concentration as NPR was evaluated in quadruplicate.

Evaluation of antiherpetic activity in vitro

The inhibitory concentration 50 (IC₅₀) was determined using a viral plaque reduction assay, according to the methodology described by Silva Mares *et al.* (30). Briefly, a confluent monolayers of Vero cells in 24-well culture plates were incubated with 25 plaque-forming units (PFU) of HSV for 1 h at 37 °C. The supernatant was discarded and fresh medium supplemented with 2 % propylene glycol and 0.32 % IgG was added. Concentrations of 187, 93.5, 46.75, 23.37, and 11.68 $\mu\text{g mL}^{-1}$ of RZ in NPR were evaluated. In addition, the IC₅₀ of the NPBco was evaluated. The cells were incubated for 48 h. Finally, the cells were fixed with methanol and stained with the Giemsa reagent. Saline phosphate buffer was used as the negative control. The IC₅₀ was that at which a 50 % reduction in PFU formation was observed compared to the 0 % reduction in the negative control. All assays were performed in triplicate for both viruses (HSV-1 KOS and HSV-2 G). The selectivity index (SI) of each sample was calculated as the ratio of CC₅₀ to IC₅₀ (31).

Statistical analysis

Statistical analysis was performed using GraphPad Prism software, and the Student's *t*-test was used to compare the means of the two groups. One-way ANOVA, followed by a

multiple comparison test, was performed to compare the means of more than two groups ($p < 0.05$).

RESULTS AND DISCUSSION

Optimization and characterization of NPE

The NPs were formulated using the nanoprecipitation technique established by Fessi *et al.* (24), which has been successfully used to load a wide variety of natural products – such as the methanolic extract of red propolis (32), the hydroalcoholic extract of *Passiflora edulis* (33), luteolin (34), and the essential oil of *Piper nigrum* L. (35) – into polymeric nanocarriers. Nanoprecipitation is based on the slow interaction between a solvent phase (SP) and a non-solvent phase (NSP) at room temperature with constant agitation. The polymer and active ingredients are dissolved in the SP, which must contain at least one solvent soluble in the NSP. However, NSP must not be able to dissolve the polymer or the active ingredient; it is usually water, and sometimes an active surfactant is added. When the two phases come into contact, the miscible solvent in the NSP diffuses from the SP into the NSP, modifying the solubility of both the polymer and active ingredient. As the concentration of the polymer in the resulting mixture exceeds its thermodynamic solubility limit, the polymer chains begin to aggregate, incorporating the active ingredient and resulting in the formation of NPs (36). The key factors controlling the formation of NPs using the nanoprecipitation technique are the active ingredient, polymer, and solubility in both phases.

Among the ideal characteristics of NPs for biological applications, the polymers should be safe and biocompatible (37, 38). The Eudragit® family of polymers includes biocompatible polymethacrylates widely used in the pharmaceutical industry for the development of drug delivery systems (39). In a previous investigation, our group evaluated the ability of four different polymers of the Eudragit family to incorporate RZ from DEJ. The following polymers were evaluated: E-100, RL-100, RS-100, and L-100 55; the Eudragit® L100-55 polymer showed the best results (40). For this work, we select Eudragit® L100-55, a copolymer composed of methacrylic acid/ethyl acrylate in a 1:1 ratio and is sensitive at $\text{pH} \geq 5.5$ (39).

The first factor that was optimized in this work was the concentration of DEJ. Three concentrations were evaluated: 0.6, 0.84, and 1.4 mg mL^{-1} (FE1, FE2, and FE3, respectively); the polymer concentration was 14 mg mL^{-1} in all cases. The three formulations presented a zeta potential from -35.4 to -41.1 mV. These values are attributed to the anionic nature of the Eudragit® L100-55 polymer due to the presence of carboxylic acid terminal groups. Kamble *et al.* stated that zeta potential values greater than or equal to ± 30 mV generate electrostatic repulsions between nanoparticles, which helps to avoid their aggregation (41). Therefore, the zeta potential values of the NPE formulations were considered suitable. The PDI values ranged from 0.169–0.239. The PDI is a measure of the homogeneity of a sample based on its size; PDI values range from 0 to 1. Sadeghi *et al.* asserted that a formulation is considered monodisperse if its PDI is < 0.3 and presents a single peak in the size distribution curve (42). Therefore, all three formulations were monodispersed. Particle size is a crucial factor; various authors consider that the ideal size for the biological application of nanoparticles is 100–300 nm, avoiding elimination by glomerular filtration and elimina-

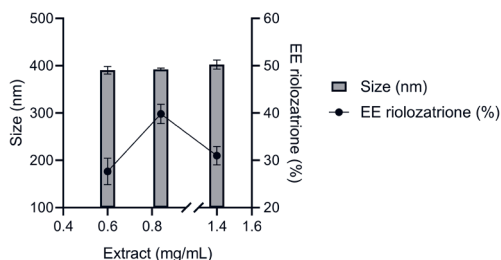


Fig. 2. Results of particle size and the encapsulation efficiency [EE (%)] of formulations with different *J. dioica* extract concentrations: 0.6 (FE1), 0.84 (FE2), and 1.4 mg mL⁻¹ (FE3). Results are presented as mean ± standard deviation, *n* = 3.

tion by macrophages (43–45). The three initial formulations had particle sizes greater than 390 nm (Fig. 2). Statistical analysis (ANOVA, *p* < 0.05) revealed no significant differences between the sizes of the formulations. Therefore, we decided to use EE as the determining factor for the selection of the formulation with which the optimization would continue. The EE results are shown in Fig. 2. Although a higher concentration of the extract was used in FE3, the EE was significantly higher in FE2. This decrease in EE may be due to the RZ/polymer ratio; it is possible that the polymer did not incorporate enough RZ, and because of its low polarity, it was lost in the process (34, 46). Because FE2 obtained the best EE, a concentration of 0.84 mg mL⁻¹ of DEJ was selected to continue optimizing the NPR.

The second factor to be optimized was the polymer concentration, which was determined to be 8 mg mL⁻¹ (FE4). A particle size of 246.45 ± 13.55 nm, PDI of 0.07 ± 0.004, and zeta potential of -30.43 ± 0.95 mV were obtained. These values are within the ideal range for biological applications. In addition, the EE increased from 39.81 ± 2.05 % in FE2 to 50.49 ± 3.11 % in FE4. The decrease in particle size and increase in EE can be attributed to the decrease in SP viscosity owing to the lower polymer concentration. Elmowafy *et al.* reported that an adequate viscosity of SP allows for a better distribution of the components in the SP, which translates into fewer aggregates and better EE (34). Considering these results, we decided to evaluate the stability of FE4; the results are presented in Table I. Statistical analysis (ANOVA, *p* < 0.05) showed no significant differences between the size and PDI of

Table I. Physicochemical characterization of polymeric nanoparticles loaded with the dichloromethane extract of *J. dioica* root (FE4) and loaded with riolozatrione (NPR)

	FE4			NPR	
	Initial	6 months	11 months	Initial	6 months
Size (nm)	246.45 ± 13.55	245.95 ± 18.02	247.4 ± 26.71	263.26 ± 14.21	268.45 ± 3.73
PDI	0.07 ± 0.04	0.09 ± 0.05	0.11 ± 0.02	0.13 ± 0.02	0.07 ± 0.04
Presence of aggregates	No	No	No	No	No

Data expressed as mean ± SD, *n* = 3.

the formulations at any of the evaluated times. No aggregates or macroscopic changes were observed in the formulations during the evaluation period. Therefore, NPE (FE4) was stable for at least 11 months after processing.

Preparation and characterization of NPR

After optimization of the NPE formulations and according to the parameters of particle size, PDI, and zeta potential mentioned above, FE4 was selected to continue the encapsulation studies of pure RZ. Elaborating a formulation with pure riolozatrione avoids the possible interference of compounds present in the extract, both in the encapsulation process and in bioactivity and cytotoxicity assays (47, 48). The obtained NPR exhibited a size of 263.26 ± 14.21 nm, Smolenski *et al.* mention that nanoparticles > 200 nm have the ability to penetrate the vaginal mucosa and reach the vaginal epithelium (49). The PDI index of the NPR was 0.13 ± 0.02 and their zeta potential was -37.16 ± 2.16 mV. This change in zeta potential with respect to FE4 may be due to the presence of cationic compounds in DEJ (41). The EE of the NPR was 89.64 ± 7.81 % and their RZC was 5.89 ± 0.33 %. This increase in EE with respect to FE4 was attributed to the absence of other hydrophobic compounds competing with RZ for incorporation into the polymer matrix. Similarly, there is no interference effect due to the excess mass, as in the case of DEJ (47). The stability results of the NPR are listed in Table I. Statistical analysis (*t*-test, $p < 0.05$) showed no significant differences between the size and PDI of the formulations 6 months after preparation. No aggregates or macroscopic changes were observed in the formulations during the evaluation period. In addition, RZC showed no significant differences after 6 months of storage (*t*-test, $p < 0.05$). Therefore, the NPR was stable for at least six months. Regarding the residual solvents, only isopropanol was present, and its concentration was well below the limits suggested by the USP (26). Chromatograms are shown in the Supplementary Material.

As part of the chemical characterization of NPR, FTIR analysis of Eudragit® L100-55 polymer, RZ, and NPR was performed; the spectra are shown in Fig. 3. In the spectrum of

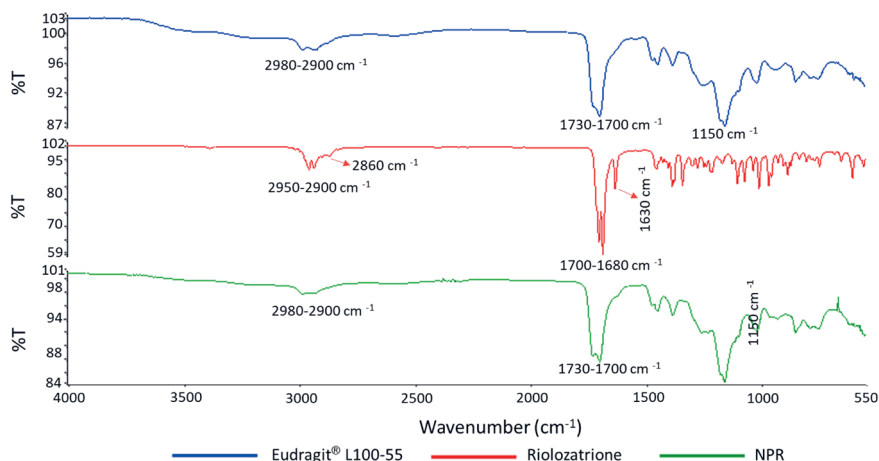


Fig. 3. FT-IR spectra of Eudragit® L100-55, riolozatrione, and polymeric nanoparticles loaded with riolozatrione (NPR), 4000 to 400 cm^{-1} .

Eudragit® L100-55, the important signals of the functional groups present in the polymeric unit of this copolymer were identified. The C-H stretching band of the alkyl groups was observed at 2932 cm^{-1} . The presence of the carbonyl group (C=O) leads to the appearance of signals in 1730 and 1700 cm^{-1} corresponding to the C=O stretching of the carboxylic acid and ester respectively. Finally, the signal at 1157 cm^{-1} corresponds to the C-O stretching of the ester. These signals agree with the spectrum of Eudragit® L100-55 obtained using attenuated total reflectance FTIR by Yu *et al.* (50). On the other hand, in the RZ spectrum, signals were observed in the regions of 2955 , 2933 , and 2866 cm^{-1} which correspond to the C-H stretching of methyl, methylene, and methine, respectively. In addition, two intense signals were observed at 1702 and 1684 cm^{-1} , which correspond to the stretching of unconjugated and conjugated C=O, respectively. In addition, a signal at 1632 cm^{-1} due to the C=C stretching of the conjugated alkene was observed. This IR spectrum was very similar to the RZ spectrum reported by Melchor-Martinez *et al.* (15). Finally, in the FTIR spectrum of the NPR, signals representative of the Eudragit® L100-55 polymer appeared, such as the O-H stretching (2982 cm^{-1}), the C=O stretching of the ester (1730 cm^{-1}), and the C=O stretching of the carboxylic acid (1700 cm^{-1}). However, in this spectrum, it is not possible to observe an intense signal at 1632 cm^{-1} corresponding to the C=C stretching of the alkene conjugated in RZ. In addition, bands indicating the formation of new compounds were not observed; therefore, it is inferred that there is only an electrostatic interaction between the polymer and RZ.

In vitro study of RZ release

In this study, we evaluated the release profile at pH 7.4, which is the pH used in cell culture; the release at pH 4.3 was also evaluated due to vaginal administration of NPR intended in the future, and the vaginal pH is slightly acidic (pH 4 to 5) (51, 52). The results of RZ release from the NPR are shown in Fig. 4. In both cases, an initial burst effect is observed in the first 15 min: $71.41 \pm 0.19\%$ of RZ is released at pH 4.3; at pH 7.4, $86.75 \pm 0.31\%$ is released. This fast release can be attributed to the presence of adsorbed RZ on the NPR surface. The release profile shows a biphasic effect after the initial burst. Sustained release of RZ is observed for 48 hours, and the final percentage release of RZ was $95.19 \pm 0.31\%$ at a pH of 7.4 and $97.53 \pm 0.94\%$ at a pH of 4.3. This biphasic release behavior was similar to that exhibited by omeprazole-loaded Eudragit® L100-55 NPs prepared by Hao *et al.* The *in vitro* release profile of omeprazole at pH 6.8 presented a rapid initial release followed by a sustained release for 48 h with a final percent release of 85% (53). At both pH values, the sustained release was observed for 48 h, and extended-release formulations have been shown to significantly improve patient adherence to treatment (54).

Although Eudragit® L100-55 is insoluble at pH < 5.5, the release of RZ at pH 4.3 according to Changning *et al.* may be due to the NPR gradually swelling, which allows the diffusion of RZ into the dissolution medium (50). As shown in Fig. 4, the initial release percentage at pH 4.3 was significantly lower than that at pH 7.4; however, as time passed, the release percentage at pH 4.3 increased until it surpassed the final release percentage at pH 7.4. Based on these results, it can be inferred that after the initial burst, the release of RZ from the NPR depends more on the deterioration of the polymeric lattice of the NPs than on the solubility of the polymer (47).

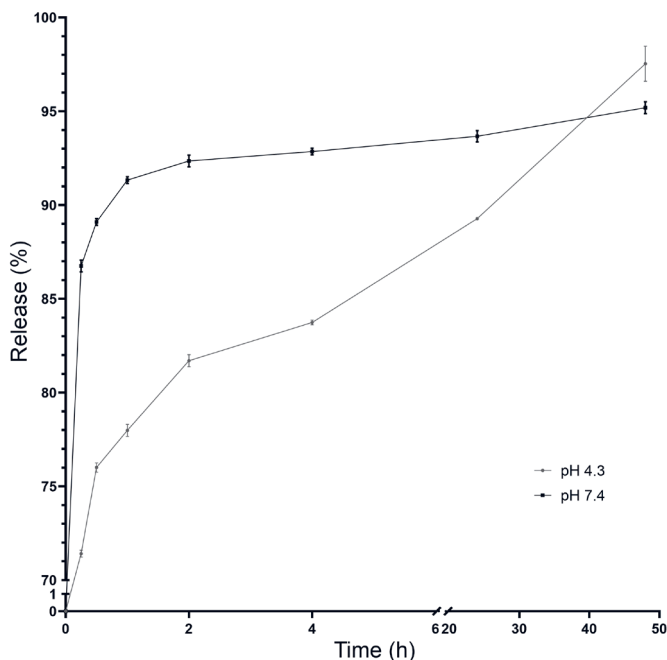


Fig. 4. Rioloatrione release profile from rioloatrione-loaded polymeric nanoparticles in buffer at pH 4.3 and 7.4. Results are presented as mean \pm standard deviation, $n = 3$.

Cell viability assessment and *in vitro* evaluation of antiherpetic activity

The antiherpetic activity assays were performed using Vero cells because of their ability to grow in monolayers and their facility to demonstrate cytopathic effects, making them a suitable cell line for viral plaque reduction assays (31). To obtain an objective selectivity index (SI) result, cell viability assays were performed using the same linear cell. Despite having an IC_{50} value, if the SI of an antiviral agent is not reported, it is worthless (31). NPR exhibited a CC_{50} value of $229 \pm 17.80 \mu\text{g mL}^{-1}$ with a dose-dependent cytotoxic effect. Fig. 5 plots the results of cell viability after the administration of $20 \mu\text{g mL}^{-1}$ RZ, ACV, NPR (equivalent to $20 \mu\text{g mL}^{-1}$ RZ), and NPBco at the same polymer concentration as NPR. The results showed that NPBco and ACV did not generate cytotoxic effects in Vero cells at the evaluated concentrations, which agreed with the GRAS classification of Eudragit[®] polymers (39) and with the reported CC_{50} for ACV in Vero cells, which was $> 1441 \text{ g mL}^{-1}$ (55). However, at the same RZ concentration, NPR led to higher cell viability than free RZ. Since the cytotoxic effect of any active compound depends largely on its form of administration, we can infer that the encapsulation of RZ; thus, its controlled release decreases its cytotoxicity (56).

NPBco did not show any detectable *in vitro* antiviral activity against HSV-1 or HSV-2 at any of the tested concentrations. This agrees with a study by Yadavalli *et al.* where the efficacy of carboxylic acid-terminated polymers in neutralizing HSV-1 and HSV-2 prior to

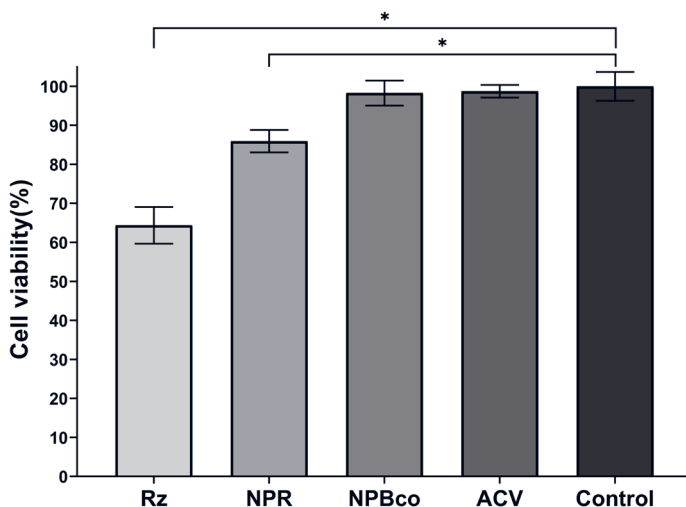


Fig. 5. Cell viability after treatment with riolozatrione (RZ), polymeric nanoparticles loaded with riolozatrione (NPR), polymeric nanoparticles not loaded (NPBco), and acyclovir (ACV) at $20 \mu\text{g mL}^{-1}$. * Statistically significant differences ($p < 0.0001$). Results are presented as mean \pm standard deviation, $n = 5$.

infection was evaluated, as well as their therapeutic activity; the results showed that Eudragit® L100-55 has no therapeutic activity against HSV-1 or HSV-2 and that its effect in neutralizing both viruses is very limited (57). The IC_{50} and SI values of the NPR against HSV-1 and HSV-2 are presented in Table II.

Indrayanto *et al.* proposed that if a compound isolated from plant material exhibits an $SI \geq 10$, it is a compound with potential activity and should be further investigated (58). Therefore, the NPR possesses potential antiherpetic activity against both HSV-1 and HSV-2. The reported SI for free RZ is 5.8 for both viruses, the NPR formulation allowed doubling of the SI for HSV-2 and almost tripling for HSV-1 (15). The slight selectivity of RZ for HSV-1 may be attributable to the phenotypic differences between the two viruses (59, 60). However, further studies are needed to elucidate the mechanism of action of RZ in detail and to determine the cause of its selectivity.

Table II. Inhibitory concentration 50 (IC_{50}) and selectivity index (SI) of polymeric nanoparticles loaded with riolozatrione (NPR) against herpes simplex virus type I (HSV-1) and II (HSV-2)

	NPR	
	HSV-1	HSV-2
IC_{50}	$14.39 \pm 0.68 \mu\text{g mL}^{-1}$	$17.58 \pm 0.59 \mu\text{g mL}^{-1}$
SI	15.91	13.02

Data expressed as mean \pm SD, $n = 4$.

CONCLUSIONS

The optimized NPR showed a biphasic release profile, with a sustained release of RZ for 48 h in the second phase. The NPR formulation exhibited improved antiherpetic activity compared to free RZ. These results are promising for future applications of this NPR formulation in vaginal *in vivo* HSV infection models.

Acknowledgments. – The authors acknowledge the valuable support of QCB Citlaly Vanessa Rodríguez Santiago who collaborated with us as part of her social service. This project was funded by the CONACYT grant number 252846 (2015) and by the UANL support program PAICYT SA 1901-21 and PAICYT 176-CS2022. Guadalupe Yazmín Solís Cruz is grateful to the Postgraduate Scholarship Program 856396 of CONACYT-Mexico.

Conflict of interest. – The authors declare no conflict of interest in the publication of this article.

Funding. – This research received no external funding.

Authors contributions. – Conceptualization, R.A-R., V.R-G. and L.P-L.; preparation of DEJ and purification of riolozatrione V.R-G. and G.S-C.; formulation, optimization, and characterization of NPR, R.A-R. and S.G-R. and G.S-C.; release profiles of NPR R.A-R. and G.S-C.; analysis of residual solvents, M.E-S.; *in vitro* evaluation, D.S-M., I.M-M. and G.S-C.; writing and original draft preparation, R.A-R. and L.P-L. and G.S-C. All authors participated in the analysis of the results and the revision of the manuscript.

Abbreviations. – ACV – acyclovir, CC – column chromatography, CC₅₀ – cytotoxic concentration 50, DEJ – dichloromethane extract of *J. dioica* root, DEMEM – Dulbecco's Modified Eagle Medium, EE – encapsulation efficiency, FBS – fetal bovine serum, GRAS – generally recognized as safe, HSV – Herpes simplex virus, IC₅₀ – inhibitory concentration 50, MP – mobile phase, NCs – nano-carriers, NPBco – polymeric nanoparticles no loaded, NPE – polymeric nanoparticles loaded with dichloromethane extract of *J. dioica* root, NPR – polymeric nanoparticles loaded with riolozatrione, NPs – polymeric nanoparticles, NSP – non-solvent phase, PDI – polydispersity index, PFU – plaque-forming units, Rz – riolozatrione, RZC – riolozatrione content, SI – selectivity index, SP – solvent phase, TLC – thin-layer chromatography.

REFERENCES

1. S. Zhu and A. Viejo-Borbolla, Pathogenesis and virulence of herpes simplex virus, *Virulence* **12**(1) (2021) 2670–2702; <https://doi.org/10.1080/21505594.2021.1982373>
2. V. W-H. Rabelo, N. C. Romeiro, I. C. N. de P. Paixão and P. A. Abreu, Mechanism of resistance to acyclovir in thymidine kinase mutants from Herpes simplex virus type 1: a computational approach, *J. Biomol. Struct. Dyn.* **38**(7) (2020) 2116–2127; <https://doi.org/10.1080/07391102.2019.1625443>
3. M. Shinomoto, T. Kasai, H. Tatebe, F. Kitani-Morii, T. Ohmichi, Y. Fujino, D. Allsop, T. Mizuno and T. Tokuda, Cerebral spinal fluid biomarker profiles in CNS infection associated with HSV and VZV mimic patterns in Alzheimer's disease, *Transl. Neurodegener.* **10**(2) (2021) Article ID 2 (3 pages); <https://doi.org/10.1186/s40035-020-00227-w>
4. J. Nissen, B. Trabjerg, M. G. Pedersen, K. Banasik, O. B. Pedersen, E. Sørensen, K. R. Nielsen, C. Erikstrup, M. S. Petersen, H. M. Paarup, P. Bruun-Rasmussen, D. Westergaard, T. F. Hansen, C. B. Pedersen, T. Werge, F. Torrey, H. Hjalgrim, P. B. Mortensen, R. Yolken, S. Brunak, H. Ullum and K. S. Burgdorf, Herpes Simplex Virus Type 1 infection is associated with suicidal behavior and first registered psychiatric diagnosis in a healthy population, *Psychoneuroendocrinology* **108** (2019) 150–154; <https://doi.org/10.1016/j.psyneuen.2019.06.015>
5. M. Harfouche, H. Maalmi and L. J. Abu-Raddad, Epidemiology of herpes simplex virus type 2 in Latin America and the Caribbean: systematic review, meta-analyses and metaregressions, *Sex. Transm. Infect.* **97** (2021) 490–500; <https://doi.org/10.1136/sextrans-2021-054972>

6. K. J. Looker, N. J. Welton, K. M. Sabin, S. Dalal, P. Vickerman, K. M. E. Turner, M.-C. Boily and S. L. Gottlieb, Global and regional estimates of the contribution of herpes simplex virus type 2 infection to HIV incidence: a population attributable fraction analysis using published epidemiological data, *Lancet Infect. Dis.* **20**(2) (2019) 240–249; [https://doi.org/10.1016/s1473-3099\(19\)30470-0](https://doi.org/10.1016/s1473-3099(19)30470-0)
7. L. A. Sadowski, R. Upadhyay, Z. W. Greeley and B. J. Margulies, Current drugs to treat infections with herpes simplex viruses-1 and -2, *Viruses* **13**(7) (2021) Article ID 1228 (12 pages); <https://doi.org/10.3390/v13071228>
8. S. Pirintsos, A. Panagiotopoulos, M. Bariotakis, V. Daskalakis, C. Lionis, G. Sourvinos, I. Karakasiliotis, M. Kampa and E. Castanas, From traditional ethnopharmacology to modern natural drug discovery: A methodology discussion and specific examples, *Molecules* **27**(13) (2022) Article ID 4060 (18 pages); <https://doi.org/10.3390/molecules27134060>
9. A. G. Atanasov, S. B. Zotchev, V. M. Dirsch, I. E. Orhan, M. Banach, J. M. Rollinger, D. Barreca, W. Weckwerth, R. Bauer, E. A. Bayer, M. Majeed, A. Bishayee, V. Bochkov, G. K. Bonn, N. Braidly, F. Bucar, A. Cifuentes, G. D'Onofrio and C. T. Supuran, Natural products in drug discovery: advances and opportunities, *Nat. Rev. Drug Discov.* **20** (2021) 200–216; <https://doi.org/10.1038/s41573-020-00114-z>
10. B. Huang and Y. Zhang, Teaching an old dog new tricks: Drug discovery by repositioning natural products and their derivatives, *Drug Discov. Today* **27**(7) (2022) 1936–1944; <https://doi.org/10.1016/j.drudis.2022.02.007>
11. E. Bautista, S. Lozano-Gamboa, M. Fragoso-Serrano, J. Rivera-Chávez and L. A. Salazar-Olivo, Jatrophenediol, a pseudoguaiane sesquiterpenoid from *Jatropha dioica* rhizomes, *Tetrahedron Lett.* **104** (2022) Article ID 154040 (3 pages); <https://doi.org/10.1016/j.tetlet.2022.154040>
12. Y. Silva-Belmares, C. Rivas-Morales, E. Viveros-Valdez, M. G. de la Cruz-Galicia and P. Carranza-Rosales, Antimicrobial and cytotoxic activities from *Jatropha dioica* roots, *Pak. J. Biol. Sci.* **17**(5) (2014) 748–750; <https://doi.org/10.3923/pjbs.2014.748.750>
13. B. A. Alanís-Garza, G. M. González-González, R. Salazar-Aranda, N. Waksman de Torres and V. M. Rivas-Galindo, Screening of antifungal activity of plants from the northeast of Mexico, *J. Ethnopharmacol.* **114**(3) (2007) 468–471; <https://doi.org/10.1016/j.jep.2007.08.026>
14. D. Silva-Mares, E. Torres-López, A. Rivas-Estilla, P. Cordero-Pérez, N. Waksman-Minsky and V. Rivas-Galindo, Plants from northeast Mexico with anti-HSV activity, *Nat. Prod. Commun.* **8**(3) (2013) 297–298; <https://doi.org/10.1177/1934578x1300800305>
15. E. M. Melchor-Martínez, D. A. Silva-Mares, E. Torres-López, N. Waksman-Minsky, G. F. Pauli, S. N. Chen, M. Niemitz, M. Sánchez-Castellanos, A. Toscano, G. Cuevas and V. M. Rivas-Galindo, Stereochemistry of a second riolozane and other diterpenoids from *Jatropha dioica*, *J. Nat. Prod.* **80**(8) (2017) 2252–2262; <https://doi.org/10.1021/acs.jnatprod.7b00193>
16. R. Ahmad, S. Srivastava, S. Ghosh and S. K. Khare, Phytochemical delivery through nanocarriers: a review, *Colloids Surf. B* **197** (2021) Article ID111389 (13 pages); <https://doi.org/10.1016/j.colsurfb.2020.111389>
17. A. Katopodi and A. Detsi, Solid lipid nanoparticles and nanostructured lipid carriers of natural products as promising systems for their bioactivity enhancement: The case of essential oils and flavonoids, *Colloids Surfaces A Physicochem. Eng. Asp.* **630** (2021) Article ID 127529 (11 pages); <https://doi.org/10.1016/j.colsurfa.2021.127529>
18. S. Waheed, Z. Li, F. Zhang, A. Chiarini, U. Armato and J. Wu, Engineering nano-drug biointerface to overcome biological barriers toward precision drug delivery, *J. Nanobiotechnol.* **20** (2022) Article ID 395 (25 pages); <https://doi.org/10.1186/s12951-022-01605-4>
19. O. Akbal Vural, Y. T. Yaman and S. Abaci, Secondary metabolite-entrapped, anti-GPA33 targeted poly-dopamine nanoparticles and their effectiveness in cancer treatment, *J. Appl. Polym. Sci.* **139** (2022) e52274 (11 pages); <https://doi.org/10.1002/app.52274>

20. A. Nair, R. Mallya, V. Suvarna, T. A. Khan, M. Momin and A. Omri, Nanoparticles-attractive carriers of antimicrobial essential oils, *Antibiotics* **11**(1) (2022) Article ID 108 (45 pages); <https://doi.org/10.3390/antibiotics11010108>
21. D. Wang, E. Mehrabi Nasab and S. S. Athari, Study effect of baicalein encapsulated/loaded chitosan-nanoparticle on allergic asthma pathology in mouse model, *Saudi J. Biol. Sci.* **28**(8) (2021) 4311–4317; <https://doi.org/10.1016/j.sjbs.2021.04.009>
22. S. Sangboonruang, N. Semakul, S. Sookkree, J. Kantapan, N. Ngo-Giang-huong, W. Khamduang, N. Kongyai and K. Tragoolpua, Activity of propolis nanoparticles against HSV-2: Promising approach to inhibiting infection and replication, *Molecules* **27**(8) (2022) Article ID 2560 (16 pages); <https://doi.org/10.3390/molecules27082560>
23. R. Castro-Ríos, E. M. Melchor-Martínez, G. Y. Solís-Cruz, V. M. Rivas-Galindo, D. A. Silva-Mares and N. C. Cavazos-Rocha, HPLC method validation for *Jatropha dioica* extracts analysis, *J. Chromatogr. Sci.* **58**(5) (2020) 445–453; <https://doi.org/10.1093/chromsci/bmaa004>
24. H. Fessi, F. Puisieux, J. P. Devissaguet, N. Ammoury and S. Benita, Nanocapsule formation by interfacial polymer deposition following solvent displacement, *Int. J. Pharm.* **55**(1) (1989) R1–R4; [https://doi.org/10.1016/0378-5173\(89\)90281-0](https://doi.org/10.1016/0378-5173(89)90281-0)
25. S. Galindo-Rodríguez, E. Allémann, H. Fessi and E. Doelker, Physicochemical parameters associated with nanoparticle formation in the salting-out, emulsification-diffusion, and nanoprecipitation methods, *Pharm. Res.* **21**(8) (2004) 1428–1439; <https://doi.org/10.1023/B:PHAM.0000036917.75634.be>
26. United States Pharmacopeia, 467, *Residual Solvents, Residual Solvents-Verification of Compendial Procedures and Validation of Alternative Procedures*, December 2020; https://www.uspnf.com/sites/default/files/usp_pdf/EN/USPNF/revisions/gc-467-residual-solvents-ira-20190927.pdf; last access date April 7, 2023.
27. S. S. Yousaf, A. Isreb, I. Khan, E. Mewsiga, A. Elhissi, W. Ahmed and M. A. Alhnan, Impact of nanosizing on the formation and characteristics of polymethacrylate films: micro- versus nano-suspensions, *Pharm. Dev. Technol.* **26** (2021) 729–739; https://doi.org/10.1080/10837450.2021.1931886/suppl_file/iphd_a_1931886_sm4082.pdf
28. J. Weng, H. H. Y. Tong and S. F. Chow, *In vitro* release study of the polymeric drug nanoparticles: development and validation of a novel method, *Pharmaceutics* **12** (2020) Article ID 732 (18 pages); <https://doi.org/10.3390/pharmaceutics12080732>
29. T. Mosmann, Rapid colorimetric assay for cellular growth and survival: Application to proliferation and cytotoxicity assays, *J. Immunol. Methods* **65**(1-2) (1983) 55–63; [https://doi.org/10.1016/0022-1759\(83\)90303-4](https://doi.org/10.1016/0022-1759(83)90303-4)
30. D. Silva-Mares, V. M. Rivas-Galindo, R. Salazar-Aranda, L. A. Pérez-Lopez, N. Waksman De Torres, J. Pérez-Meseguer and E. Torres-Lopez, Screening of north-east Mexico medicinal plants with activities against herpes simplex virus and human cancer cell line, *Nat. Prod. Res.* **33**(10) (2019) 1531–1534; <https://doi.org/10.1080/14786419.2017.1423300>
31. P. Cos, A. J. Vlietinck, D. Vanden Berghe and L. Maes, Anti-infective potential of natural products: How to develop a stronger *in vitro* “proof-of-concept,” *J. Ethnopharmacol.* **106**(3) (2006) 290–302; <https://doi.org/10.1016/j.jep.2006.04.003>
32. L. Farias Azevedo, P. da Fonseca Silva, M. Porfírio Brandão, L. Guerra da Rocha, C. F. S. Aragão, S. A. S. da Silva, I. C. C. M. Porto, I. D. Basílio-Júnior, E. J. da S. Fonseca, M. A. B. Fidelis de Moura and T. G. do Nascimento, Polymeric nanoparticle systems loaded with red propolis extract: a comparative study of the encapsulating systems, PCL-Pluronic versus Eudragit® E100-Pluronic, *J. Apic. Res.* **57**(2) (2018) 255–270; <https://doi.org/10.1080/00218839.2017.1412878>
33. J. S. F. Alves, A. M. Dos Santos Silva, R. M. Da Silva, P. R. F. Tiago, T. G. De Carvalho, R. F. De Araújo Júnior, E. P. De Azevedo, N. P. Lopes, L. De Santis Ferreira, E. C. Gavioli, A. A. Da Silva-Júnior and S. M. Zucolotto, *In vivo* antidepressant effect of *Passiflora edulis* f. *flavicarpa* into cationic nanoparticles:

- improving bioactivity and safety, *Pharmaceutics* **12**(4) (2020) Article ID 383 (19 pages); <https://doi.org/10.3390/pharmaceutics12040383>
34. M. Elmowafy, N. A. Alhakamy, K. Shalaby, S. Alshehri, H. M. Ali, E. F. Mohammed, N. K. Alruwaili and A. Zafar, Hybrid polylactic acid/Eudragit L100 nanoparticles: A promising system for enhancement of bioavailability and pharmacodynamic efficacy of luteolin, *J. Drug Deliv. Sci. Technol.* **65** (2021) Article ID 102727 (13 pages); <https://doi.org/10.1016/j.jddst.2021.102727>
 35. M. Zhang, B. Qiu, M. Sun, Y. Wang, M. Wei, Y. Gong and M. Yan, Preparation of black pepper (*Piper nigrum* L.) essential oil nanoparticles and its antitumor activity on triple negative breast cancer *in vitro*, *J. Food Biochem.* **46** (2022) e14406 (13 pages); <https://doi.org/10.1111/jfbc.14406>
 36. E. Piacentini, B. Russo, F. Bazzarelli and L. Giorno, Membrane nanoprecipitation: From basics to technology development, *J. Memb. Sci. Res.* **654** (2022) Article ID 120564 (17 pages); <https://doi.org/10.1016/j.memsci.2022.120564>
 37. Y. W. Huang, M. Cambre and H. J. Lee, The toxicity of nanoparticles depends on multiple molecular and physicochemical mechanisms, *Int. J. Mol. Sci.* **18**(12) (2017) Article ID 2702 (13 pages); <https://doi.org/10.3390/ijms18122702>
 38. J. Wen, Y. Lv, Y. Xu, P. Zhang, H. Li, X. Chen, X. Li, L. Zhang, F. Liu, W. Zeng and S. Sun, Construction of a biodegradable, versatile nanocarrier for optional combination cancer therapy, *Acta Biomater.* **83** (2019) 359–371; <https://doi.org/10.1016/j.actbio.2018.11.009>
 39. J. Dos Santos, G. S. da Silva, M. C. Velho and R. C. R. Beck, Eudragit®. A versatile family of polymers for hot melt extrusion and 3D printing processes in pharmaceuticals, *Pharmaceutics* **13**(9) (2021) Article ID 1424 (36 pages); <https://doi.org/10.3390/pharmaceutics13091424>
 40. A. G. Rocha, G. Y. Solís-Cruz, V. Rivas-Galindo, L. Pérez-López, O. Portillo-Castillo, S. Galindo-Rodríguez and R. Álvarez-Román, Aplicación de nanopartículas poliméricas para extraer metabolitos del extracto de raíz de *Jatropha dioica*, *Rev. Mex. Inv. Prod. Nat.* **1**(1) (2022) 46.
 41. S. Kamble, S. Agrawal, S. Cherumukkil, V. Sharma, R. V. Jasra and P. Munshi, Revisiting zeta potential, the key feature of interfacial phenomena, with applications and recent advancements, *Chemistry-Select* **7**(1) (2022) e202103084 (40 pages); <https://doi.org/10.1002/slct.202103084>
 42. R. Sadeghi, S. G. Etamad, E. Keshavarzi and M. Haghshenasfard, Investigation of alumina nanofluid stability by UV-vis spectrum, *Microfluid Nanofluidics* **18** (2015) 1023–1030; <https://doi.org/10.1007/s10404-014-1491-y>
 43. A. R. Bilia, V. Piazzini, L. Risaliti, G. Vanti, M. Casamonti, M. Wang and M. C. Bergonzi, Nanocarriers: A successful tool to increase solubility, stability and optimise bioefficacy of natural constituents, *Curr. Med. Chem.* **26**(24) (2019) 4631–4656; <https://doi.org/10.2174/0929867325666181101110050>
 44. X. Cai, X. Liu, J. Jiang, M. Gao, W. Wang, H. Zheng, S. Xu and R. Li, Molecular mechanisms, characterization methods, and utilities of nanoparticle biotransformation in nanosafety assessments, *Small* **16** (2020) Article ID 1907663 (19 pages); <https://doi.org/10.1002/sml.201907663>
 45. N. Yadav, S. Parveen and M. Banerjee, Potential of nano-phytochemicals in cervical cancer therapy, *Clin. Chim. Acta* **505** (2020) 60–72; <https://doi.org/10.1016/j.cca.2020.01.035>
 46. N. A. Rivero-Segura and J. C. Gomez-Verjan, *In silico* screening of natural products isolated from Mexican herbal medicines against COVID-19, *Biomolecules* **11**(2) (2021) Article ID 216 (12 pages); <https://doi.org/10.3390/biom11020216>
 47. L. Han, Y. Fu, A. J. Cole, J. Liu and J. Wang, Co-encapsulation and sustained-release of four components in ginkgo terpenes from injectable PELGE nanoparticles, *Fitoterapia* **83**(4) (2012) 721–731; <https://doi.org/10.1016/j.fitote.2012.02.014>
 48. J. L. Dahlin, D. S. Auld, I. Rothenaigner, S. Haney, J. Z. Sexton, J. W. M. Nissink, J. Walsh, J. A. Lee, J. M. Strelow, F. S. Willard, L. Ferrins, J. B. Baell, M. A. Walters, B. K. Hua, K. Hadian and B. K. Wagner, Nuisance compounds in cellular assays, *Cell Chem. Biol.* **28**(3) (2021) 356–370; <https://doi.org/10.1016/j.chembiol.2021.01.021>

49. M. Smoleński, B. Karolewicz, A. M. Gołkowska, K. P. Nartowski and K. Małolepsza-Jarmołowska, Emulsion-based multicompartiment vaginal drug carriers: From nanoemulsions to nanoemulgels, *Int. J. Mol. Sci.* **22**(12) (2021) Article ID 6455 (39 pages); <https://doi.org/10.3390/ijms22126455>
50. C. Yu, Q. Litke, Q. Li, P. Lu, S. Liu, F. Diony, J. Gong, C. Yang and S. Liu, Targeted delivery of sodium metabisulfite (SMBS) by pH-sensitive Eudragit L100-55 nanofibrous mats fabricated through advanced coaxial electrospinning, *J. Mater. Sci.* **57** (2022) 3375–3395; <https://doi.org/10.1007/s10853-021-06785-2>
51. A. M. dos Santos, S. G. Carvalho, V. H. S. Araujo, G. C. Carvalho, M. P. D. Gremião and M. Chorilli, Recent advances in hydrogels as strategy for drug delivery intended to vaginal infections, *Int. J. Pharm.* **590** (2020) Article ID 119867 (12 pages); <https://doi.org/10.1016/j.ijpharm.2020.119867>
52. G. B. Löwhagen, E. Bonde, U. Forsgren-Brusk, B. Runeman and P. Tunbäck, The microenvironment of vulvar skin in women with symptomatic and asymptomatic herpes simplex virus type 2 (HSV-2) infection, *J. Eur. Acad. Dermatology Venereol.* **20**(9) (2006) 1086–1089; <https://doi.org/10.1111/j.1468-3083.2006.01729.x>
53. S. Hao, B. Wang, Y. Wang, L. Zhu, B. Wang and T. Guo, Preparation of Eudragit L 100-55 enteric nanoparticles by a novel emulsion diffusion method, *Colloids Surf. B.* **108** (2013) 127–133; <https://doi.org/10.1016/j.colsurfb.2013.02.036>
54. J. A. Romley, Z. Xie, T. Chiou, D. Goldman and A. L. Peters, Extended-release formulation and medication adherence, *J. Gen. Intern. Med.* **35** (2020) 354–356; <https://doi.org/10.1007/s11606-019-05275-1>
55. T. Priengprom, T. Ekalaksananan, B. Kongyingyoes, S. Suebsasana, C. Aromdee and C. Pientong, Synergistic effects of acyclovir and 3,19-isopropylideneandrographolide on herpes simplex virus wild types and drug-resistant strains, *BMC Complement. Altern. Med.* **15** (2015) Article ID 56 (8 pages); <https://doi.org/10.1186/s12906-015-0591-x>
56. G. Nocca, G. D'avenio, A. Amalfitano, L. Chronopoulou, A. Mordente, C. Palocci and M. Grigioni, Controlled release of 18- β -glycyrrhetic acid from core-shell nanoparticles: Effects on cytotoxicity and intracellular concentration in hepg2 cell line, *Materials* **14**(14) (2021) Article ID 3893 (13 pages); <https://doi.org/10.3390/ma14143893>
57. T. Yadavalli, S. Mallick, P. Patel, R. Koganti, D. Shukla and A. A. Date, Pharmaceutically acceptable carboxylic acid-terminated polymers show activity and selectivity against HSV-1 and HSV-2 and synergy with antiviral drugs, *ACS Infect. Dis.* **6** (2020) 2926–2937; <https://doi.org/10.1021/acsinfectdis.0c00368>
58. G. Indrayanto, G. S. Putra and F. Suhud, *Validation of In-vitro Bioassay Methods: Application in Herbal Drug Research*, in *Profiles of Drug Substances, Excipients and Related Methodology* (Eds. A. Bakheit and K. Florey), 1st ed., Academic Press, Cambridge 2021, pp. 273–307.
59. E. Trybala, J.-Å. Liljeqvist, B. Svennerholm and T. Bergström, Herpes simplex virus types 1 and 2 differ in their interaction with heparan sulfate, *J. Virol.* **74**(19) (2000) 9106–9114; <https://doi.org/10.1128/jvi.74.19.9106-9114.2000>
60. J. S. Aguilar, G. V. Devi-Rao, M. K. Rice, J. Sunabe, P. Ghazal and E. K. Wagner, Quantitative comparison of the HSV-1 and HSV-2 transcriptomes using DNA microarray analysis, *Virology* **348**(1) (2006) 233–241; <https://doi.org/10.1016/j.virol.2005.12.036>